

LABORATORY EXPERIMENTS IN COLD TEMPERATURE  
ROCK DEFORMATION

by

LAURA JANE VAN ALST

A THESIS

Presented to the Department of Geological Sciences  
and the Graduate School of the University of Oregon  
in partial fulfillment of the requirements  
for the degree of  
Master of Science  
December 2011

THESIS APPROVAL PAGE

Student: Laura Jane Van Alst

Title: Laboratory Experiments in Cold Temperature Rock Deformation

This thesis has been accepted and approved in partial fulfillment of the requirements for the Master of Science degree in the Department of Geological Sciences by:

Alan Rempel	Chairperson
Joshua Roering	Member
Rebecca Dorsey	Member

and

Kimberly Andrews Espy	Vice President for Research & Innovation/Dean of the Graduate School
-----------------------	---

Original approval signatures are on file with the University of Oregon Graduate School.

Degree awarded December 2011

© 2011 Laura Van Alst

## THESIS ABSTRACT

Laura Jane Van Alst

Master of Science

Department of Geological Sciences

December 2011

Title: Laboratory Experiments in Cold Temperature Rock Deformation

The physical weathering of rock in cryogenic regions through a process called ice segregation is important for understanding subglacial processes, landscape evolution and cold region engineering. Ice segregation was examined by freezing water-saturated cores of Eugene Formation sandstone at temperatures between  $-15^{\circ}$  and  $-2^{\circ}$  C. Cores between  $-8^{\circ}$  and  $-5^{\circ}$  C took 30-45 minutes to crack, while cores at warmer or cooler temperatures took either more than 90 minutes or did not crack at all. Numerical modeling shows that cores break under isothermal conditions. The results of this study suggest that previous models in which temperature gradients are held responsible for driving flow towards growing cracks are incomplete. I introduce a new model of ice segregation to explain how premelted liquids from smaller pores can migrate and contribute to the growth of large cracks. This dissertation includes unpublished material.

## CURRICULUM VITAE

NAME OF AUTHOR: Laura Jane Van Alst

### GRADUATE AND UNDERGRADUATE SCHOOLS ATTENDED:

University of Oregon, Eugene  
University of New Mexico, Albuquerque  
University of New Hampshire, Durham

### DEGREES AWARDED:

Master of Science, Geological Sciences, 2011, University of Oregon  
Bachelor of Science, Earth and Planetary Sciences, 2009,  
University of New Mexico

### PUBLICATIONS:

Gutzler, G. S., and L. Van Alst (2010), Interannual variability of wildfires and summer precipitation in the Southwest, *New Mex. Geol.*, 32, 22-24.

## ACKNOWLEDGMENTS

I would like to thank Alan Rempel, Becky Dorsey and Josh Roering for their valuable insights and support while preparing this manuscript. The preliminary experiments for this project were conducted by Zakk Carter as part of the UCORE program in the summer of 2010. Additional laboratory work was conducted by Naomi Mecham. This work was made possible in part by the National Science Foundation, Office of Polar Programs and the University of Oregon Geologic Sciences department.

## TABLE OF CONTENTS

Chapter	Page
I. INTRODUCTION.....	1
II. METHODS.....	8
Experimental Design.....	9
Thermal Model.....	15
III. RESULTS .....	19
Thin Sections .....	19
Thermal Model.....	21
Laboratory Experiments.....	21
Control Groups.....	27
IV. DISCUSSION.....	29
Eugene Formation .....	29
Berea Sandstone and Tyee Formation .....	36
V. CONCLUSION.....	38
APPENDIX: CORE COOLING MODEL DERIVATION .....	40
REFERENCES CITED.....	43

## LIST OF FIGURES

Figure	Page
1. Liquid produced by ice-particle interactions ( <b>A</b> ) and the Gibbs-Thomson effect ( <b>B</b> ). These are the two sources of premelted liquid in partially-frozen porous media.....	3
2. Chart of the total weight of each core through time as it was saturated with “vacuum soak”, “beaker soak”, and “vacuum then water” method.....	10
3. The average results of six cores of Eugene Formation that were used to test three different methods of saturation.....	11
4. This set of photographs shows the progression of ice segregation deformation seen in the one inch cores of Eugene Formation Sandstone. ....	15
5. Thin section photographs of Eugene Formation, Tyee Formation and Berea Sandstone under cross-polarized and plane polarized light.....	20
6. Thermal model showing the temperature of the rock core as a function of time.....	22
7. Experimental data that show the average breaking time for Eugene Formation cores at temperatures between 0 and -15°C. ....	23
8. Experimental data as shown in <b>Figure 7</b> (Eugene Formation), showing a close up of break times less than 300 minutes.....	25
9. This figure shows the deformation of a core of Eugene Formation through times $t_0$ , $t_1$ and $t_2$ .....	32
10. The distribution of crack lengths in a porous rock with two temperatures $T_1$ and $T_2$ denoted.....	34

## LIST OF TABLES

Table	Page
1. Saturation data for six cores of Eugene Formation using three different methods. ....	13
2. Rock Core Breaking Data. ....	24
3. Comparison of averaging schemes. ....	26
4. Values of constants used in the thermal model.....	42

## CHAPTER I

### INTRODUCTION

Landscapes in cold regions are shaped by weathering processes associated with the growth of ice crystals. The formation of ice can cause soil heave and the cracking of rocks, which create hazards such as rock falls in cold regions [*Gruber and Haeblerli, 2007*]. Recent studies have used cold region rock deformation that results in scree slopes as a paleoclimate indicator [*Hales and Roering, 2005, 2007*]. Further study of mechanical weathering helps engineers design safe infrastructure that combat the hazards caused by unstable slopes and soil heave [*Coussy, 2005*]. Although glacial processes are traditionally credited as the most effective erosion and weathering mechanisms in nature [*Hallet et al., 1996*], there are actually many cold region weathering processes occurring around the margins of glaciers that contribute to the erosional effectiveness of glaciers. In turn, glaciers also increase the effectiveness of many cold region weathering mechanisms, both by eroding soils and vegetation to expose bedrock to the elements, and by providing a source of liquid water. In this thesis, I use laboratory experiments and models to gain insight into one of the most important mechanisms that contribute to cold region weathering: cracking that is associated with the growth of ice crystals in porous rock.

Ice crystal growth is not the only mechanism for cracking rocks in cold regions. Rapid temperature changes can cause a rock to fracture in a process called thermal shock [*Hall, 1999*]. As the rock is cooled, the molecules within the rock come closer together and the density of the rock increases. Rocks have relatively low thermal conductivities,

which means that it takes a relatively long time for the interior of a rock to equilibrate with the temperature of its surroundings. While the center of the rock remains warm, the contracting rock around it experiences stresses associated with the change in density that can be strong enough to fracture the rock [Hall and André, 2001]. Thermal shock causes cracks to develop perpendicular to each other on the exposed faces of the rock [Hall and André, 2001]. Frost cracking does not depend on the presence of liquid water; this makes it unique amongst cold region weathering mechanisms.

The fundamental processes that break rocks as water freezes within microcracks and pores are closely related to those that cause frost heaving [Washburn, 1980; Taber, 1929]. Frost heaving is commonly seen when an unconsolidated ground surface bulges upwards from the formation of ice lenses. A layer of liquid water remains between growing ice crystals and mineral grains in the substrate due to ice-particle interactions and the Gibbs-Thomson effect [Dash *et al.*, 2006; Rempel, 2007]. The thin film of liquid that remains even after the temperature is below the freezing point is called a premelted film. Although solutes within the pore water can cause a depression in freezing temperatures, the presence of premelted liquid is not dependent on these effects [Dash *et al.*, 2006]. The interactions between molecules near the boundary between a particle and an ice crystal cause premelted films to form [Hansen-Goos and Wettlaufer, 2010]. These films coat particle and ice surfaces and are denoted in **Figure 1** with an **A**. Another type of premelting forms macroscopic menisci along contacts with particles and ice crystals with a radius of curvature that decreases as it gets colder. This phenomenon are referred to as the Gibbs-Thomson or curvature effects and accounts for the majority of the

premelted liquid contained in porous media at temperatures just below freezing. These effects are labeled in **Figure 1** with a **B**.

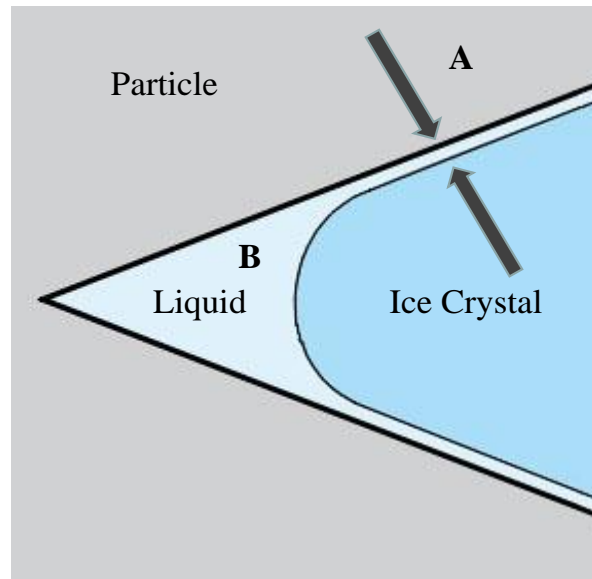


**Figure 1.** Liquid produced by ice-particle interactions (**A**) and the Gibbs-Thomson effect (**B**). These are the two sources of premelted liquid in partially-frozen porous media. Figure adapted from Wettlaufer and Worster, 2006.

Frost heave occurs when the temperature at the surface decreases below the freezing point. Although it is commonly assumed by those outside of the ice-segregation research community that the source of water in frost heaving is locally derived, it can actually be transported out of an unfrozen region toward growing “segregated” ice lenses along the conduits provided by premelted films [McGreevey and Whalley, 1985]. As ice forms in the pore space, phase equilibria require that the water pressure in the premelted liquid be lower than that in the surrounding ice crystals. The pressure difference becomes larger as temperatures drop further below the normal “bulk” melting temperature. The pressure gradients that develop when temperature gradients are present cause unfrozen

water from a reservoir, most commonly in warmer sediments that are above the melting point, to flow towards a growing lens of ice [Rempel, 2007]. In frost heaving, the mechanics of nanoscale films and the interactions between particles and ice control the macroscale deformational processes [Rempel, 2007]. A thorough understanding of the physics behind frost heaving led to the recognition that a similar “ice segregation” process can occur in rocks [Walder and Hallet, 1985; Washburn, 1980].

Ice segregation occurs when ice forms within the pores of a rock and draws liquid water towards growing ice crystals in a process similar to frost heaving. The rock grains and the ice growing within pores and microcracks are coated with premelted films at a temperature below the freezing point of water [Wettlaufer and Worster, 2006]. Premelted films are thickest when the ice is close to its melting temperature and decrease in thickness as the temperature decreases. Ice segregation depends on the transport of water along premelted films towards a growing ice crystal. Cracks develop when the ice pressure in pores exceeds a threshold strength. Liquid within the premelted film flows into the extended pore and is crystallized by the growing ice. This creates a low liquid pressure and draws more premelted water towards the ice crystal. If the temperature is too low, the premelted films cannot effectively transport water. However, if the temperature is too close to the freezing point there is not enough of a pressure difference between the ice and water to propagate a crack and induce flow [Dash *et al.*, 2006]. This delicate balance suggests that ice segregation should only occur within a small range of temperatures [Hales and Roering, 2005]. Although previous theories assume that a reservoir of liquid water and a strong thermal gradient are required to induce ice

segregation [*Walder and Hallet, 1985*], my data suggest that crack growth can occur long after isothermal conditions are established. Premelted water is able to flow from small cracks towards larger cracks where the stress concentration induced by the growing ice crystals at the crack tip exceeds the strength of the rock. This is how ice segregation can break apart rocks in just a single freezing event.

In frost heaving experiments the heaving pressure exerted by the ice against the sediments has been measured at nearly 30 MPa [*Hallet et al., 1991*]. Given typical flaw sizes, these pressures are at least twice those required for the tensile fracture of the strongest rocks [*Hallet et al., 1991*]. Therefore, as long as there is a water source, cracks or pores for ice to form in, and a sufficiently low temperature, rocks should break under the force of ice segregation. The propagation of cracks within brittle materials is dependent on the pressures exerted over the crack surface as well as the crack size (*Walder and Hallet, 1985*). The crack tip can propagate when the stress intensity factor at the tip of cracks,  $\sigma_I$ , exceeds the fracture toughness of the rock,  $\sigma_C$ .

Ice segregation may be the most important form of physical weathering in cryogenic regions but it is poorly understood amongst the general public. Many educational resources and introductory textbooks still incorrectly say the 9% density difference between water and ice causes rock damage in a process called frost wedging [*Hallet, 2006*]. Although it is not impossible for frost wedging to occur under ideal conditions [*Davidson and Nye, 1985; Matsuoka, 2001*], there are many difficulties with applying this hypothesis to the natural world. Rocks are difficult to saturate in natural

environments and rocks that undergo frost wedging need to have pores that contain upwards of 90% liquid water by volume for any significant increase in stress to occur from the volumetric expansion caused by the growth of ice [Hallet, 2006]. If rocks are less saturated, air pockets can collapse to accommodate the change in volume. The volumetric expansion of ice growing in a crack is not an effective mechanism for fracturing bedrock because it would increase the liquid pressure of the premelted films along the ice-particle boundary. This would increase the flow of liquid water away from the growing ice crystals and toward a part of the rock where ice can freeze with a minimal amount of stress [Hallet, 2006]. The numerical cooling model in the results section shows this behavior. In nature, pores and cracks that allow water to enter a rock can also accommodate the flow of premelted films out of the rock during ice segregation [Hallet, 2006]. Although this process has traditionally been attributed to thermal gradients in the rock driving the flow of liquid water, my laboratory and model results demonstrate that ice segregation can also occur in an isothermal regime.

In the methods section that follows, I describe the laboratory methods that I used to dry and subsequently saturate cores. I support my choice of laboratory methods with evidence from preliminary studies. Next, I present my laboratory results and demonstrate that ice segregation occurs most rapidly at an intermediate range of temperatures between -5 and -8 °C. The discussion section interprets the findings of the laboratory results in terms of a new conceptual model of ice segregation under isothermal conditions. I describe how small cracks that are below the threshold for fracture propagation may be a source of premelted liquid that migrates to longer cracks that are actively growing

segregation ice and propagating. I also describe how the permeability, distribution of pore and crack sizes and the background confining stress of the rock may have contributed to keeping the Berea Sandstone and Tyee Formation samples from experiencing ice segregation deformation.

## CHAPTER II

### METHODS

Samples of Eugene Formation sandstone were obtained from an outcropping near the Autzen bike bridge at the University of Oregon. This sandstone was selected because of its proximity to the laboratory and the homogeneity within the outcrop. I visually inspected the grain size, weathering, friability and composition of the sandstone along the length of the outcrop and determined that it was homogenous. I collected large pieces of Eugene Formation that were already dislodged from the outcrop to bring back to the lab for coring. One-inch cores of Berea Sandstone were purchased and cut into 2-inch long cores. The Tyee Formation along the Oregon coast also contains sandstones of varying compositions and grain sizes. I collected large samples of Tyee formation on Route 38 approximately 10.6 miles east of the intersection of highway 101 and 38 in Reedsport, OR. The samples were collected from an abandon quarry near the confluence of the Charlotte Creek drainage and the Umpqua River where the Tyee Formation outcrops in steep cliffs immediately south of Route 38. We cored samples of Tyee and Eugene Formation that were one inch in diameter and 2-3 inches long using a modified drill press with a rock coring bit. All of the cores we collected were from rocks that showed no macroscopic signs of deformation or cracking. The purpose of collecting cores from the Eugene Formation, Berea Sandstone and the Tyee Formation was to study the effects of ice segregation on these porous sandstones under the controlled conditions of the laboratory.

## Experimental Design

We used a procedure for preparing cores that limited variations in size, shape, solutes or initial rock saturation on our results. We cored between ten and thirty one inch samples from each large piece of Eugene and Tyee Formation that we have collected from the source. The cores were washed in tap water to remove any rock residue from the coring process and dried in an oven at 80° C for 24 hours. The drying time was chosen following a series of experiments that showed that the cores stopped losing weight after 12 hours in the oven. Twenty-four hours was used to guarantee the sample was completely dry, even if it had a slightly different porosity or initial saturation from the test drying experiments. We chose a temperature of 80° C because it was the warmest temperature that did not visually affect the color or texture of the rock. Experimental trials with warmer temperatures yielded cores that were discolored and may have been altered. After the cores had dried, they were marked with a sample number, weighed with an AND electronic scale EK-1200i and allowed to cool overnight to room temperature.

Three different methods of saturating the rock cores were compared in a controlled experiment to determine the most efficient method. A “vacuum soak” was performed by placing the samples in a vacuum vessel, filling the vessel with water, and drawing a vacuum several times [**Figure 2**]. Bubbles trapped in the pores of the rock samples were enlarged by creating a vacuum. When the pressure was increased to atmospheric, bubbles were expelled from the rock samples and replaced by water overlying the rock sample. Unfortunately, water evaporated from inside the vessel faster

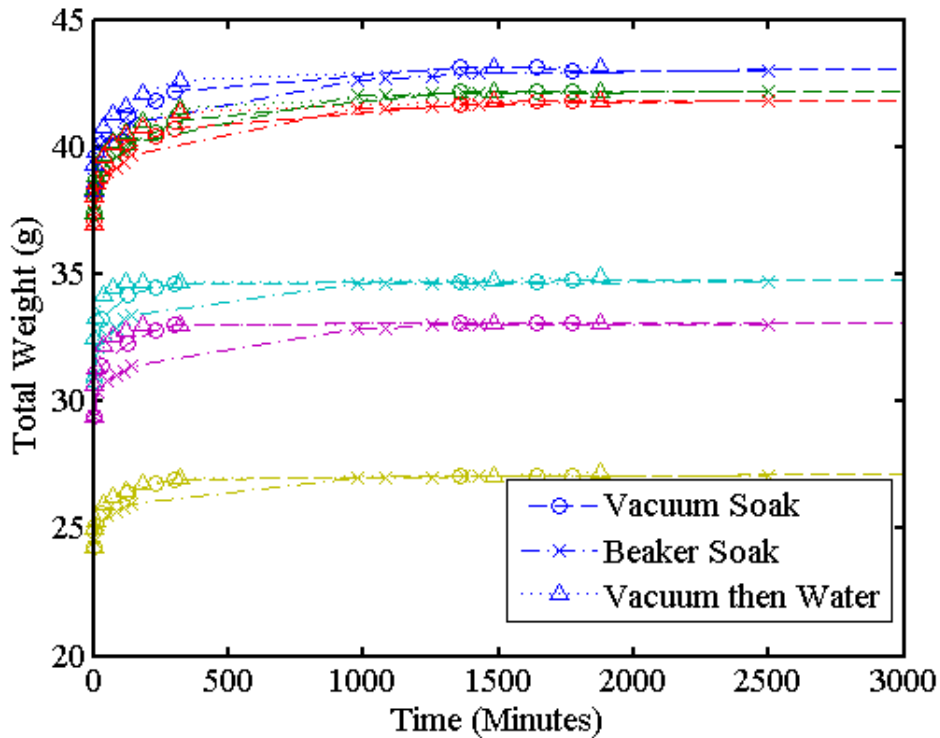


**Figure 2.** Chart of the total weight of each core through time as it was saturated with “vacuum soak”, “beaker soak”, and “vacuum then water” method. Since the same six cores were used for all three experiments I can compare between saturation experiments. Each core is plotted with a different colored line. Symbols are used to denote the saturation method used.

than the vacuum pump could remove vapors. This resulted in a relatively weak vacuum that was only moderately effective at saturating the cores. Next we tried the “vacuum then water” method by pulling a vacuum with dry samples in the vessel and adding the water under vacuum [Figure 2]. This created a much stronger vacuum because there was no water in the vessel to evaporate. When I added the water under vacuum, the rock absorbed more water in a shorter period of time than in the vacuum soak case.

Nevertheless, this method still required that the cores soak in water for several days before they achieved full saturation. The final method of “water soak” involved leaving the cores submerged in water at atmospheric pressure for several days [Figure 2].

Although the vacuum gauge recorded relative pressures amongst all three methods, the gauge was not accurate enough to give specific pressures.

Although the vacuum soak and vacuum then water methods saturated cores faster, all three methods led to approximately the same saturation levels after three days [Figure 3]. Since the same six cores of Eugene Formation were used in all three experiments, we experienced some cracking and flaking when the cores were dried between the “beaker soak” and “vacuum then water” experiments. Figure 2 shows how each rock core

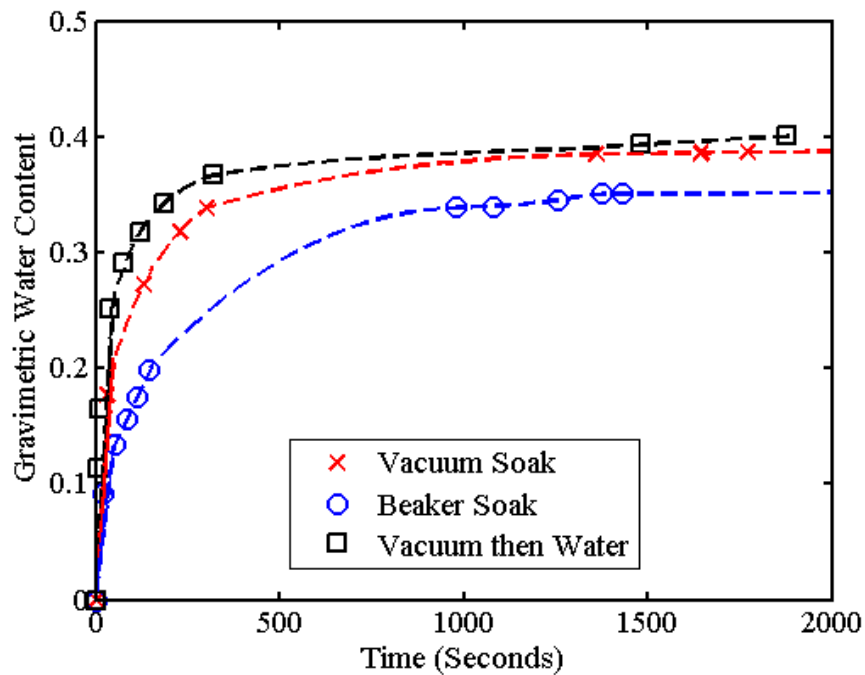


**Figure 3.** The average results of six cores of Eugene Formation that were used to test three different methods of saturation. The gravimetric water content is the weight of water divided by the weight of the dried core. “Vacuum soak” cores were placed in water and a vacuum was pulled to saturate. “Beaker soak” cores were placed in water with no vacuum. “Vacuum then water” cores were placed under vacuum and water was added under vacuum.

reached approximately the same final rock weight. Although the cores were dried for 24 hours between experiments, it is possible we still had residual water left in the core that account for the differences in the gravimetric water content. **Table 2** shows that the final weight of all three saturation methods led to nearly the same combined water and rock weight. When the cores were removed for weighing in the vacuum experiments, the newly formed cracks were holding a disproportionate amount of water which oozed from the rock. The nearly 10% difference in gravimetric water content between the beaker soak and vacuum experiments may have been due to the absorption of water in these cracks or residual water [**Figure 3**]. The final weights of all three saturation methods were within 0.2 grams of each other, and often identical for the different saturation methods. We choose the “beaker soak” method because it was the simplest method of saturating cores. It is also the method that best replicates processes that we are trying to study in the natural world.

The saturated weight and volume of each core were measured before the cores were placed in the cold bath. The saturated weight was taken on the AND electronic scale EK-1200i. The volume of the solid rock and the water within its pores was estimated using two graduated cylinders and the water displacement method. A graduated cylinder was filled with a known initial volume of water. The rock core was added to the cylinder to bring the level of water to a new, slightly larger final volume. The initial volume was subtracted from the final volume of water, to give the volume of the rock in the liquid. Using the dry weight, saturated weight, and the volume of the saturated rock I

Beaker Soak Method												
Time in Minutes Since Saturation Began												
Core #	0	20	52	84	114	144	980	1080	1256	1375	1430	2498
1	38.7	39.7	40.1	40.4	40.6	40.9	42.6	42.7	42.8	42.9	42.9	43
2	37.8	38.8	39.3	39.6	39.8	40.1	42	42	42.1	42.1	42.1	42.2
3	37.5	38.4	39	39.2	39.4	39.7	41.5	41.5	41.6	41.7	41.7	41.8
4	31	32.1	32.6	32.9	33.2	33.4	34.6	34.6	34.6	34.6	34.6	34.7
5	29.4	30.4	30.8	31	31.2	31.4	32.9	32.9	33	33	33	33
6	24.5	25.2	25.5	25.7	25.8	26	27	27	27	27.1	27.1	27.1
Vacuum then Water												
Time in Minutes Since Saturation Began												
Core #	0	5	10	40	75	120	185	320	1480	1880		
1	38.3	39.3	39.8	40.8	41.3	41.6	42.1	42.6	43.1	43.1		
2	37.4	38.4	38.9	39.7	40.2	40.6	41	41.5	42.2	42.2		
3	37	38.1	38.6	39.6	40.1	40.5	40.8	41.4	41.8	41.8		
4	30.7	32.5	33.3	34.2	34.5	34.7	34.7	34.7	34.8	34.9		
5	29.4	30.7	31.3	32.2	32.6	32.8	33	33	33.1	33.1		
6	24.3	25	25.3	26	26.3	26.5	26.8	27	27.1	27.2		
Vacuum Soak												
Time in Minutes Since Saturation Began												
Core #	0	30	130	230	300	1360	1645	1770	5700			
1	38.4	40.1	41.2	41.8	42.2	43.1	43.1	43	43.1			
2	37.4	39.1	40.1	40.6	41	42.2	42.2	42.2	42.2			
3	37.1	38.8	39.9	40.4	40.7	41.7	41.8	41.8	41.8			
4	30.8	33.2	34.2	34.5	34.6	34.7	34.7	34.8	34.8			
5	29.4	31.4	32.3	32.8	33	33.1	33.1	33.1	33.1			
6	24.3	25.6	26.4	26.8	26.9	27.1	27.1	27.1	27.2			

**Table 1.** Saturation data for six cores of Eugene Formation using three different methods. Shown are weights in grams of rock cores. Weight at time zero is the dry weight of the core. The weights at later times are the weight of the dry core plus weight of water absorbed

determined the volume of water absorbed by each rock. I also determined a minimum porosity of the rocks. The porosity of the Eugene formation was determined experimentally. I conducted the experiments on rocks that were saturated and with ice segregation testing. I used these cores because we had a saturated weight and total volume already calculated. Combined with this test for porosity we can calculate how much of the pore space was saturated during the ice segregation experiments. The cores were oven dried for 24 hours at 80 °C. Then the core was carefully powdered in a metal bowl to prevent the loss of rock dust. The rock powder was transferred to a graduated cylinder where it was weighed again using the AND electronic scale. Thirty mL of water was added to the rock powder and the mixture was stirred to eliminate air bubbles. The final volume of rock powder and water was recorded to give the volume of the rock powder. This allowed us to calculate the porosity of the rock and also the saturation level

To determine how quickly a rock core will deform in cold temperatures, samples were submerged in a sealed plastic bag for up to 2 days in a cold bath, kept at a fixed temperature. Between 4 and 6 samples of Eugene Formation were run at temperatures of -2, -3, -5, -6, -8, -10, -11, -13, and -14 °C [Table 2]. The Neslab circulating bath can accurately maintain a temperature in the cold bath to within 0.1° C. Cores were checked every 15 minutes to determine the extent of deformation by visual inspection of the outside of the core. If the core had cracks that were visible to the naked eye it was considered “cracked” in the results. Examples of cracked cores are shown in **Figure 4**, photos B, C and D. If a core was so deformed that the shape of the circular core was compromised and the original surface was not intact as shown in **Figure 4**, photo E, I considered it fully “deformed” and the core was removed from the cold bath. Cores were

checked every 15 minutes to track the deformation through time while minimizing the effect of being examined at room temperature during deformation. The results of these experiments are presented in the Results section under Laboratory Experiments.

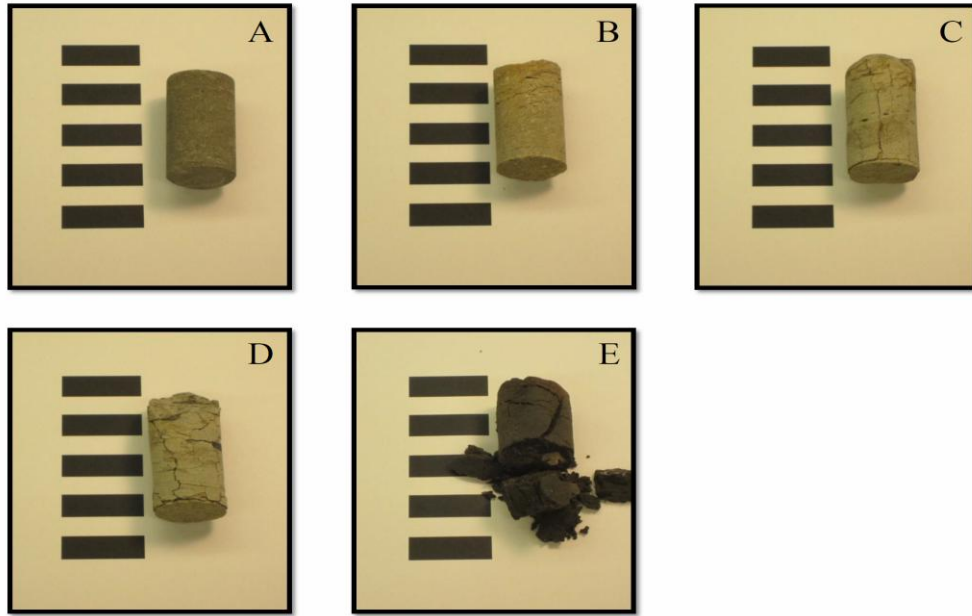


**Figure 4.** This set of photographs shows the progression of ice segregation deformation seen in the one inch cores of Eugene Formation Sandstone. Each black bar is exactly one centimeter thick. Core A is a fully intact core that has not experienced deformation from ice segregation. Core B has small cracks around the outside of the core. Core C has cracked the full length of the core and a ring crack has formed around the base of the core. Core D has progressed far enough that the surface of the core is starting to flake off. Core E represents the last stage of ice segregation where the core has completely deteriorated and can no longer hold its own shape.

#### Thermal Model

A thermal model was used to explore how thermal gradients effect ice segregation in a rock core. Model parameters were chosen from experimental values and coefficients reported in the ice- segregation literature [Rempel, 2007]. We did not take into account the thermal cooling from the ends of the cores, but focused on the center of the core as modeled in cross section with a temperature gradient along the radius of a circle. The

governing equations describe changes in pore fluid pressure, and temperature along the radius of the core half way between the two ends of the core through time. By representing the center of the core, this model describes the region of the core that would take the longest time to cool from ambient temperature to the temperature of the cold bath. I use this model to predict the time at which the center of core is cooled to within 0.1 °C of the circulating bath.

The model is based on the conservation of mass and energy within a closed system. The conservation of mass **[Equation 1]** describes how a change in ice saturation  $S_i$  with time  $t$  can induce the flow of fluids within the core because of the change in density from liquid  $\rho_l$  to ice  $\rho_i$ . The second term in this equation denotes the change in air saturation  $S_a$  with time, which also induces the flow of water within the core. The Darcy transport rate  $\mathbf{u}$  describes how liquid water flows along a pressure gradient. The Porosity  $\phi$  is defined as the volume of pore spaces over the total volume of the rock.

$$(\rho_i - \rho_l)\phi \frac{\partial S_i}{\partial t} - \rho_l\phi \frac{\partial S_a}{\partial t} = -\rho_l(\nabla \cdot \mathbf{u}) \quad \text{[Equation 1]}$$

The effective thermal conductivity  $K_e$  **[Equation 2]**, the volumetrically averaged heat capacity  $\overline{\rho C}$  **[Equation 3]** and the Darcy transport rate  $\mathbf{u}$  **[Equation 4]** are defined as

$$K_e = K_i^{\phi S_i} K_l^{\phi S_l} K_a^{\phi S_a} K_p^{1-\phi} \quad \text{[Equation 2]}$$

$$\overline{\rho C} = [\rho_i\phi S_i h_i + \rho_l\phi S_l h_l + \rho_a\phi S_a h_a + \rho_p(1 - \phi)h_p] \quad \text{[Equation 3]}$$

$$\mathbf{u} = -\frac{k_l(S_l)}{\mu_l} \nabla P_l \quad \text{[Equation 4]}$$

Using the parameters defined above, the conservation of energy can be rewritten as

$$\bar{\rho}C \frac{\partial T}{\partial t} - \rho_i L \phi \frac{\partial S_i}{\partial t} \approx -\rho_i C_i \mathbf{u} \cdot \nabla T + \nabla \cdot (K_e \nabla T) \quad [\text{Equation 5}]$$

Where T is temperature and L is the latent heat. The first term in **Equation 5** describes how the heat content varies in proportion to the changes in temperature of the saturated rock as a function of time according to the volumetrically averaged heat capacity. The second term accounts for the latent heat released as the ice saturation  $S_i$  evolves. The third term uses  $\mathbf{u}$ , the Darcy transport rate, to describe how heat is transported by the flow of water through the rock. Finally, the last term describes the conduction of heat down the temperature gradient. **Equation 5** was simplified by the assumption that the advective transport of heat through air pockets is minimal and can be neglected.

The final governing **Equation 6** states that the amount of air in the rock core remains constant during freezing. To simplify this equation we assumed that air does not dissolve in the liquid. We also assume that the pressure of the liquid water in the core is the same as the air pressure. With these modifications, the governing equation for air saturation can be written as

$$\rho_a S_a = \text{Constant} \quad [\text{Equation 6}]$$

where the density of air is assumed to follow the ideal gas law

$$\rho_a = \frac{P_a}{RT} \quad [\text{Equation 7}]$$

where R is the gas constant.

The equations presented here are valid when the core is below the temperature at which ice forms. At temperatures above the freezing point there is zero ice saturation and no latent heat released. Using these conditions to simplify **Equations 1** and **5** I find

$$-\rho_l \phi \frac{\partial S_a}{\partial t} = -\rho_l (\nabla \cdot \mathbf{u}) \quad \text{[Equation 8]}$$

$$\bar{\rho} C \frac{\partial T}{\partial t} \approx -\rho_l C_l \mathbf{u} \cdot \nabla T + \nabla \cdot (K_e \nabla T) \quad \text{[Equation 9]}$$

The Saturation of ice, water and air were calculated using

$$S_i + S_l + S_a = 1 \quad \text{[Equation 10]}$$

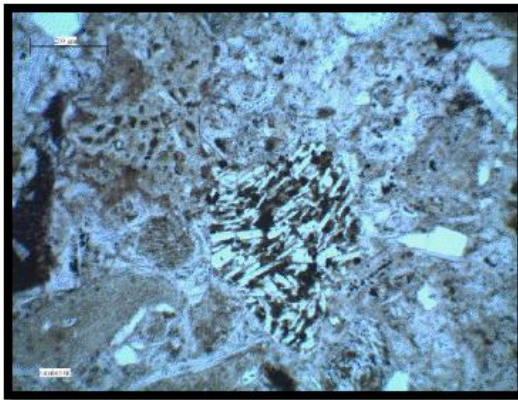
Further discussion of the equations used and their derivation can be found in the appendix.

## CHAPTER III

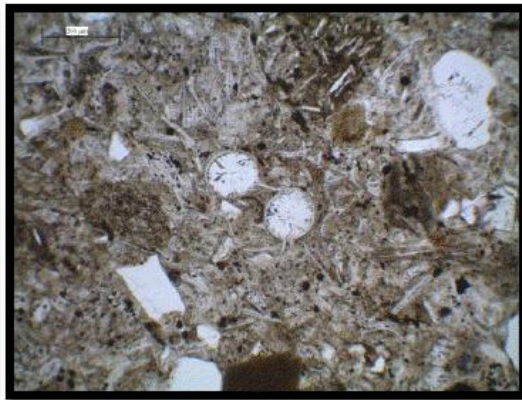
### RESULTS

#### Thin Sections

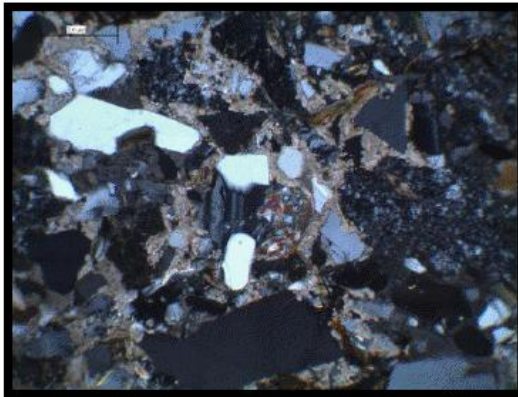
Thin sections of three different sandstones used in rock cracking experiments were made by Wagner Petrographic. Thin section analysis of the Eugene Formation samples reveals an immature volcanoclastic sandstone composed of volcanic lithic fragments, plagioclase feldspar, altered volcanic ash and glass, pumice, andesite, and minor amounts of detrital pyroxene, biotite, muscovite, small marine fossils and opaque minerals [**Figure 5**]. The lithic grains are so altered they are difficult to distinguish from each other and in areas they form a pseudo-matrix. A minor but persistent clay film has formed along the boundaries of some lithic fragments. Although the rock is composed mainly of lithic fragments, there are also quartz and feldspar grains present. In some places where feldspar grains are in contact with lithic grains, a low temperature reaction has taken place to alter the grain boundary of the feldspar to clay. The Eugene Formation can be classified as a lithic arenite because of the relative abundance of lithics compared to quartz and feldspar grains. There is no evidence of calcite or silica cementation in this sandstone. Clay films within the Eugene Formation bind grains together and act as a very weak type of cement. Given the weak, altered state of the lithic fragments and weak clay film cementation, the Eugene formation probably has the lowest tensile strength of the three sandstones examined in this thesis. Unfortunately, the pore sizes in the Eugene Formation were too small to be imaged using a petrographic microscope. I estimated the pore size of this rock to be approximately equal to 1 to 10  $\mu\text{m}$  based on the smallest visible grains within the rock.



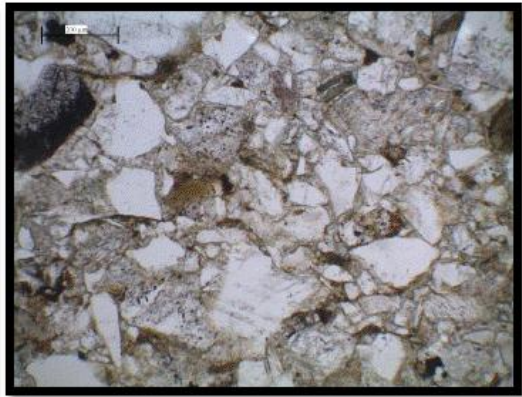
Eugene Formation (cross-polarized)



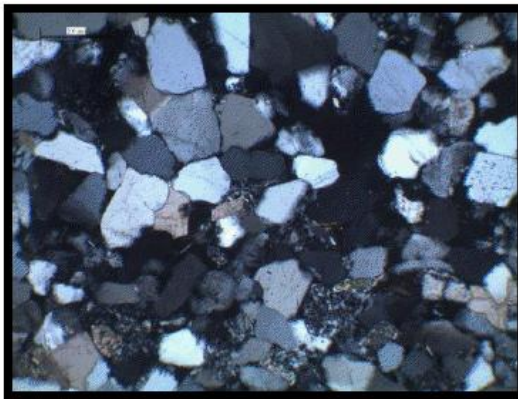
Eugene Formation (plane polarized)



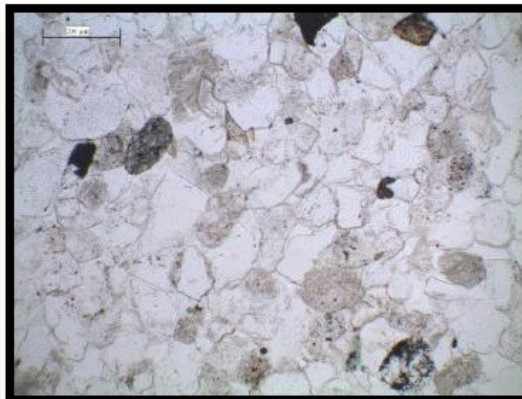
Tyee Formation (cross-polarized)



Tyee Formation (plane polarized)



Berea Sandstone (cross-polarized)



Berea Sandstone (plane polarized)

**Figure 5.** Thin section photographs of Eugene Formation, Tyee Formation and Berea Sandstone under cross-polarized and plane polarized light. Scale bar in upper left corner of photographs equals 200  $\mu\text{m}$ .

The Tyee Formation has a slightly larger abundance of quartz and feldspar grains compared to the Eugene Formation. This sandstone can be classified as a lithic to sub-lithic arenite. The grains are mainly composed of subrounded lithic fragments with a large abundance of biotite and muscovite [**Figure 5**]. Grains of polycrystalline quartz indicate that at least one parent rock of the Tyee Formation was metamorphosed in a shear zone. There are minor clay films around lithic grains. The most important discovery in the thin section analysis of the Tyee sandstone is the pervasive calcite cementation holding grains together. The Tyee formation has a larger tensile strength than the Eugene Formation due to the calcite cementation.

The Berea Sandstone is a compositionally mature quartz arenite. It is composed entirely of quartz grains which are well rounded [**Figure 5**]. It has small patches of calcite cement that may have formed from a chemical reaction associated with quartz replacement. The Berea sandstone has an abundance of silica cementation between quartz grains. This makes the Berea Sandstone very strong because both the grains and the cement are composed of quartz.

#### Thermal Model

The thermal modeling of the freezing Eugene formation was conducted to determine the time at which the rock core was completely frozen and when the temperature of the rock core had equilibrated with the temperature of the circulating bath. **Figure 6** shows the temperature of the rock as a function of time since submersion in the circulating bath. I choose  $-15^{\circ}\text{C}$  for the thermal model because that was the coldest temperature at which we froze rock cores. Rocks that were frozen at warmer temperatures

should reach an isothermal state faster than these results indicate. This model shows the maximum time the cores took to reach thermal equilibrium in the circulating bath. The dashed blue line on **Figure 6** indicates that pore ice was distributed throughout the core. The rock was completely frozen after 3 minutes and isothermal after approximately 6 minutes.

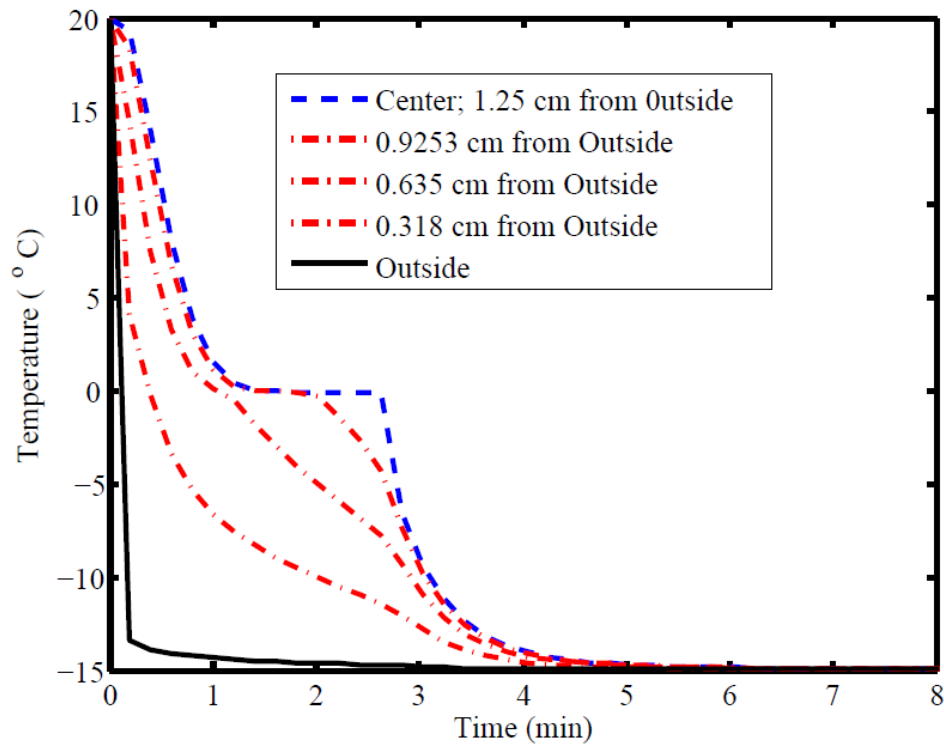


**Figure 6.** Thermal model showing the temperature of the rock core as a function of time. The temperature evolution of five points along the radius from the center of the core to the outside edge of the core is given.

### Laboratory Experiments

Freezing experiments were conducted using three types of sandstone that showed two different types of behavior. The Eugene Formation shows a clear trend in rock



crack times. The Tyee Formation and the Berea Sandstone showed no visible deformation at any temperature between -15 and -3 °C. **Figure 8** shows a close up of rock cracking times less than 300 minutes for the Eugene Formation.

Sample Number	Temperature (° C)	Dry Weight (g)	Saturated Weight (g)	Volume (ml)	Crack Time (min)
EF-11-75	-2	5.3	61.4	29	1100*
EF-11-76	-2	54.5	60.7	28	1100*
EF-11-77	-2	54.2	61.7	30	1100*
EF-11-78	-2	54.2	61.2	28.2	1100*
EF-11-79	-2	52.8	59.7	26.5	1100*
EF-11-49	-3	50.4	57.2	22	1100*
EF-11-50	-3	44.7	51.1	24	1100*
EF-11-63	-3	47.5	53.7	24	195
EF-11-64	-3	47.7	53.6	24	1100*
EF-11-73	-3	53.4	59.9	28	300
EF-11-74	-3	56.1	62.9	29	90
EF-11-21	-5	40.3	45	20.2	45
EF-11-22	-5	47.6	53.1	22.5	30
EF-11-23	-5	54.9	60.5	27.3	45
EF-11-24	-5	43.7	52.1	23	45
EF-11-12	-6	36.1	40.7	17	30
EF-11-13	-6	36	40.7	17.7	45
EF-11-14	-6	43.8	48.8	19.8	30
EF-11-15	-6	41	45.7	21.9	120
EF-11-16	-8	51.7	57.8	26.2	120
EF-11-17	-8	52.5	58	28	120
EF-11-18	-8	51.1	57.2	27.2	120
EF-11-19	-8	49.8	56.3	26.7	120
EF-11-20	-8	55.5	60.7	28	45
EF-11-1	-10	46.2	51.7	25.8	150
EF-11-2	-10	52.4	57.5	21.6	30
EF-11-3	-10	53.5	60.1	28	90
EF-11-4	-10	49	54.9	28	105
EF-11-41	-13	46.4	52.6	22.9	220
EF-11-42	-13	42.7	48	22.9	220
EF-11-45	-13	35.9	40.8	16.2	220
EF-11-46	-13	46.2	52.2	22	220
EF-11-48	-13	37.6	42.8	22.9	1100*
EF-11-43	-14	37.6	42.8	20.1	1100*
EF-11-67	-14	34.6	39.1	19.8	1100*
EF-11-68	-14	44.3	50.1	22.5	1100*
EF-11-69	-14	54.5	60.4	28	165
EF-11-70	-14	52.5	58.9	28	1100*

**Table 2.** Rock Core Breaking Data. The \* following a cracking time of 1100 minutes indicates that the Eugene Formation core never broke.

**Figure 7** was modified to average in the effects of a core that never cracked by taking the inverse of the inverse time to crack. While I can use all of the data I collected with this method, even the infinite cracking times, it tends to skew average rock cracking times towards shorter times. This skew towards shorter times does not have a significant impact on the results because rocks were cracking between 30 and 150 minutes while the thermal model shows that it only takes 13.5 minutes for the core to become essentially isothermal [**Figure 6**].

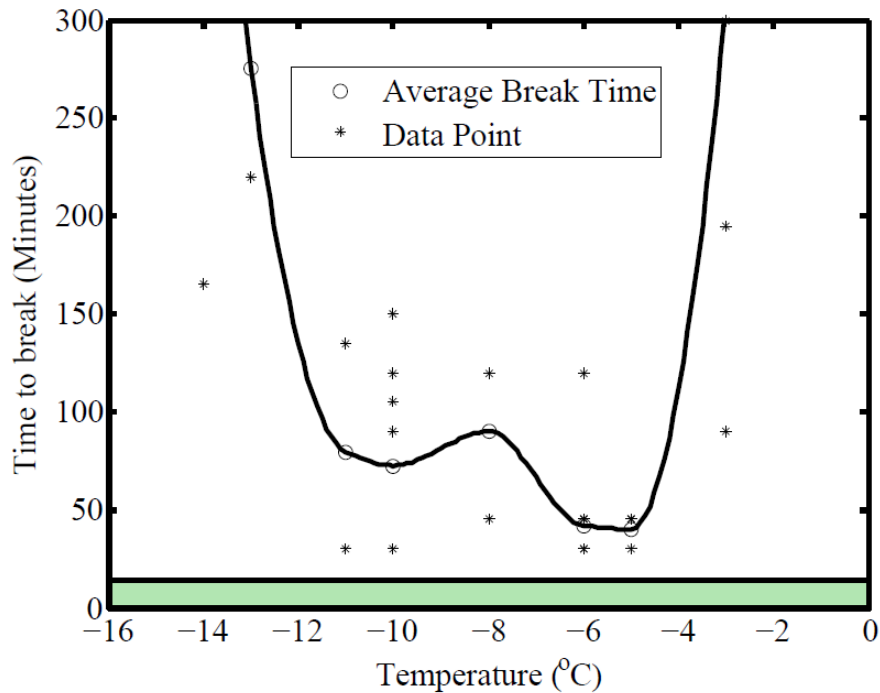


**Figure 8.** Experimental data as shown in **Figure 7** (Eugene Formation), showing a close up of break times less than 300 minutes.

I used a non-traditional averaging method to capture the behavior observed in my rock cracking results. I found that most rocks at temperatures close to 0 or -15 ° C did not break. If I was to plot my results as a function of average break times, I would not be able

to display the full data set of broken and unbroken rock times in my figure. Instead, I choose to plot the inverse of the average inverse breaking times. This allows me to average times for cores that never broke with the times of cores that did. I compare the results of my experiments using the inverse inverse averaging scheme and the mean average of broken cores without the unbroken core results in **Table 3**. The trends in the data from both schemes show clearly that rock cores closest to -2 and -15 ° C took longer to break than cores between -5 and -11 ° C.

Temperature	(Mean of 1/Break Time) <sup>-1</sup>	Mean of Break Time
-2	Infinite	N/A
-3	306	195
-5	40	41
-6	429	54
-8	90	105
-10	73	99
-11	79	114
-13	275	220
-14	825	165
-15	1024	340

**Table 3.** Comparison of averaging schemes. The mean of 1/(1/break time) is the inverse inverse method that is plotted on the graph. The Mean of Break Time is the average break time of only the cores that broke, it does not include data from cores that didn't break.

I calculated the porosity and water Saturation of a Eugene Formation core through a rock powdering method. The porosity of the rock was calculated using the volume of the saturated intact core (total volume) and the volume of the rock powder (volume of particles). The volume of voids was the defined as the difference between the saturated intact core and the volume of the rock powder. I calculated a porosity of 0.24 for a Eugene Formation rock core. I used the saturated and dry weight of the rock core and a water density of 1 g/cm<sup>3</sup> to calculate the volume of water in the saturated rock core.

Using the volume of water in the rock core and the porosity, I calculated that at the time of submersion into the cold bath, the rock had a water saturation of 0.98.

### Control Groups

Additional experiments were conducted to test our hypothesis that the deformation resulted from ice segregation. We cored, cleaned and baked the Eugene Formation cores at 80 °C for 24 hours using the same methodology as the experimental cores. Instead of saturating the cores with water, one control group was sealed in plastic immediately after being removed from the oven. The cores were allowed to cool to room temperature overnight before being placed in the Neslab circulating bath at a range of temperatures between -15 and -2°C for two days. This dry rock core control group did not undergo any associated deformation.

A separate control group was prepared by coring, cleaning, and baking but this group was saturated with ethylene glycol. Ethylene glycol is the main component in antifreeze solution and the liquid that circulates in the Neslab circulating bath. During some of the Eugene Formation rock core breaking experiments, the cores became accidentally contaminated with the ethylene glycol solution. This control was necessary to rule out interactions between the ethylene glycol solution and the rock cores that might result in breaking. The results of the Ethylene glycol control showed minimal damage with ethylene glycol at room temperatures and in -15 °C circulating bath. Rock cores developed a single, minor, crack that in one case was able to propagate through the core. Most of the deformation caused by the ethylene glycol was minor and easily

distinguishable from the more severe ice segregation deformation which left rocks flaking and crumbling.

## CHAPTER IV

### DISCUSSION

#### Eugene Formation

The rock-cracking data summarized in **Figure 7** can be combined with the thermal modeling to evaluate mechanisms of cold region weathering. The experimental results indicate that temperatures below  $-2\text{ }^{\circ}\text{C}$  were needed before core breakage was observed. As the temperature decreased further, the average break time first decreased and then remained nearly constant at  $90 \pm 50$  minutes for cold-bath temperatures between  $-5$  and  $-11\text{ }^{\circ}\text{C}$ . At colder temperatures the cores took over 150 minutes break. Trends in the data offer insight into the potential causes of rock cracking.

As noted earlier, one cold region mechanical weathering mechanism is thermal shock. This differs from other mechanisms because it does not depend on the presence of liquid water. Thermal shock occurs due to the expansion or contraction of the rock with extreme temperature gradients. To test for the presence of thermal shock in my rock core deformation experiments I used a control experiment with completely dry cores of Eugene Formation. If thermal shock contributed to the deformation noted in my experiments I should see cracking in the completely dry cores when I submerge them in the cold circulating bath. However, I detected no deformation in the cores even with the circulating bath at the coldest experimental temperature ( $-15\text{ }^{\circ}\text{C}$ ). This is strong evidence against the mechanism of thermal shock creating the deformation in the Eugene Formation cores. Further evidence comes from the cracking times noted in the rock-

cracking data in **Table 2**. If thermal shock was occurring in the Eugene Formation cores, it would happen quickly after the cores were submerged in the circulating bath. Instead we see that the cores take at least 30 minutes to break. According to the thermal modeling results, the core has reached an isothermal state by this time. With this evidence, I can confidently rule out thermal shock as the mechanism that deformed the cores of Eugene Formation.

Fracturing due to the volumetric expansion of water from liquid to solid, called frost wedging, is often credited with cold region deformation. In the past 25 years it has lost support among researchers studying cold region weathering [*Walder and Hallet, 1986*]. Even so, it is a process that can sometimes occur in natural environments so I will address it. According to the theory of frost wedging, ice growth within pores during freezing propagates cracks through the rock core. Therefore, the damage should occur at the same time as the water is freezing into ice. According to the thermal model, the transition from liquid to solid water is complete for the entire core 7.5 minutes after submersion in the circulating bath [**Figure 7**]. This implies that if frost wedging were occurring in the Eugene Formation, I should see cracks in the rock propagating for 7.5 minutes after the rock core is submerged in the circulating bath. After 7.5 minutes the rock core is completely frozen, and with little remaining liquid water to freeze, the frost wedging theory requires all deformation to stop. Instead I see that no deformation occurred in the first 30 minutes of being submerged in the circulating bath. This finding is inconsistent with frost wedging. Additionally, I find deformation between 30 and 150 minutes after submersion [**Figure 6**]. These times are long after the liquid water in the core has frozen, so the phase change from liquid to solid cannot be the sole cause of the

deformation in the Eugene Formation cores. This effectively rules out frost wedging as the mechanism of deformation in the Eugene Formation.

The established theory of ice segregation provides only a partial explanation of the physics associated with the rock-breaking results of the Eugene Formation. The flow of premelted liquids towards segregation ice is driven by a pressure gradient associated with the intermolecular interactions between the ice and particle surface. As the temperature gets colder a pressure gradient drives flow through premelted liquids towards the segregation ice. At relatively warm temperatures around  $-2\text{ }^{\circ}\text{C}$  the results indicate that the rock does not break or takes a very long time to break [Figure 7]. This is due to the relatively weak pressure exerted by the ice against the pore walls at temperatures only slightly below  $0\text{ }^{\circ}\text{C}$ . At very cold temperatures such as  $-14\text{ }^{\circ}\text{C}$  the rock cores also take a very long time to break [Figure 7]. Even when the pressure gradient in the liquid is strong, the film of premelted liquid is very thin and inhibits the flow of premelted liquid towards the segregation ice. The rapid breaking times of core in the range of  $-5$  to  $-11\text{ }^{\circ}\text{C}$  [Figure 7] indicate that the pore pressure is high enough to propagate cracks and premelted liquid is thick enough to accommodate flow that supplies ice growth..

A thermal model of the ice core used to predict when the samples submerged in the circulating bath achieved a nearly isothermal state. In my experiments, cores at room temperature were placed into a cold bath at a constant colder temperature. The thermal profile evolved over time with cooling beginning at the outer radius and the interior cooling slowly over time. To determine when the rock became isothermal, I am using the time at which the center of the rock core reaches  $0.1\text{ }^{\circ}\text{C}$  of the circulating cold bath

temperature. I picked this value because the circulating bath is accurate to 0.1 °C and temperatures changes less than this are occurring throughout the duration of the experiment. The time when the center of the rock core reaches 0.1 °C is approximately 800 seconds or 13.5 minutes [Figure 6].

The presence of ice segregation in an isothermal regime requires a new explanation for the source of liquid water. I propose that premelted water stored in small pores and cracks within the rock is being transported towards larger cracks as ice segregation occurs. As the temperature of rock decreases, the larger cracks are able to form ice crystals while the smaller cracks experience surface-energy effects that inhibit the growth of ice crystals and cause water to remain liquid [Figure 9:  $t_0$ ]. As ice

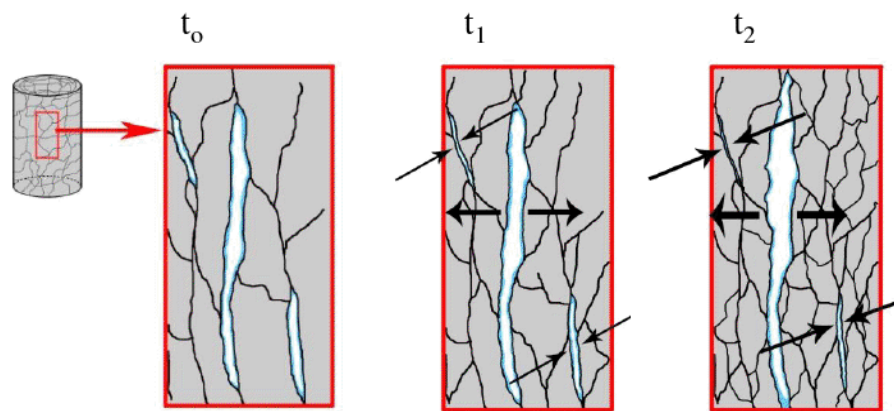


**Figure 9.** This figure shows the deformation of a core of Eugene Formation through times  $t_0$ ,  $t_1$  and  $t_2$ .  $t_0$ : One inch core of Eugene Formation is shown after the initial freezing with ice crystals in the center of all cracks.  $t_1$ : In the intermediate stage of freezing small cracks are closing and large cracks are opening. Large cracks are growing by the flow of water in premelted films along fractures and pores in the core.  $t_2$ : Eventually the large cracks can overcome the stress intensity at the fracture tip and propagate through the core. Premelted films have transported liquid away from small cracks, causing them to close.

segregation continues, large cracks in the rock propagate and become longer while smaller cracks lose water and do not grow [Figure 9:  $t_1$  and  $t_2$ ]. Large cracks can eventually intersect with each other and the surface of the core to significantly deform the rock.

The propagation of cracks within a rock depends on a number of factors such as the critical stress intensity factor,  $\sigma_{IC}$ , and the length of the crack,  $a$ . The critical stress intensity factor is a property of the rock which depends greatly on the composition of cement and grains and the shape and orientation of pores in the rock. The pressure of the ice against the sides of the crack is  $P_i$ . When the stress intensity factor, defined as the pressure of the ice against the crack walls times the square root of the crack length ' $a$ ', exceeds some critical stress intensity factor,  $\sigma_{IC}$ , the crack will propagate and become longer. The equation for the stress intensity can be written as

$$\sigma_I \propto (P_i - P_0)\sqrt{a} \quad \text{[Equation 11]}$$

Cracks that are longer will start to propagate first because the stress intensity factor is scaled by the square root of the crack length. Shorter cracks have to wait until the pressure of the ice against the crack walls is much greater in order to break. The physics of crack propagation can also explain where liquid water may be migrating from to cause segregation ice to form in larger cracks under isothermal conditions.

The propagation of large cracks without a reservoir of liquid water under isothermal conditions requires a new explanation. I will consider two cases in which the core is either at a temperature slightly less than  $0^\circ \text{C}$ ,  $T_1$ , or a temperature well below  $0^\circ \text{C}$ ,  $T_2$  [Figure 10]. At  $T_1$ , the segregation ice can exert enough pressure on the sides of

any crack size to the right of the  $T_1$  line to propagate a fracture. Cracks sizes to the left of the  $T_1$  line are too small to be able to induce fracture. Instead they provide a source of premelted liquid to the growing segregation ice forming in large cracks. At cooler temperatures such as  $T_2$ , every crack size to the right of the  $T_2$  line can propagate. This is a much larger proportion of the cracks than at warmer temperatures. At cooler temperatures, the distribution of cracks to the left of the  $T_2$  line is much smaller. There are fewer small cracks to provide a source of water for the segregation ice growing in large cracks. This conceptual model predicts that isothermal ice segregation can only

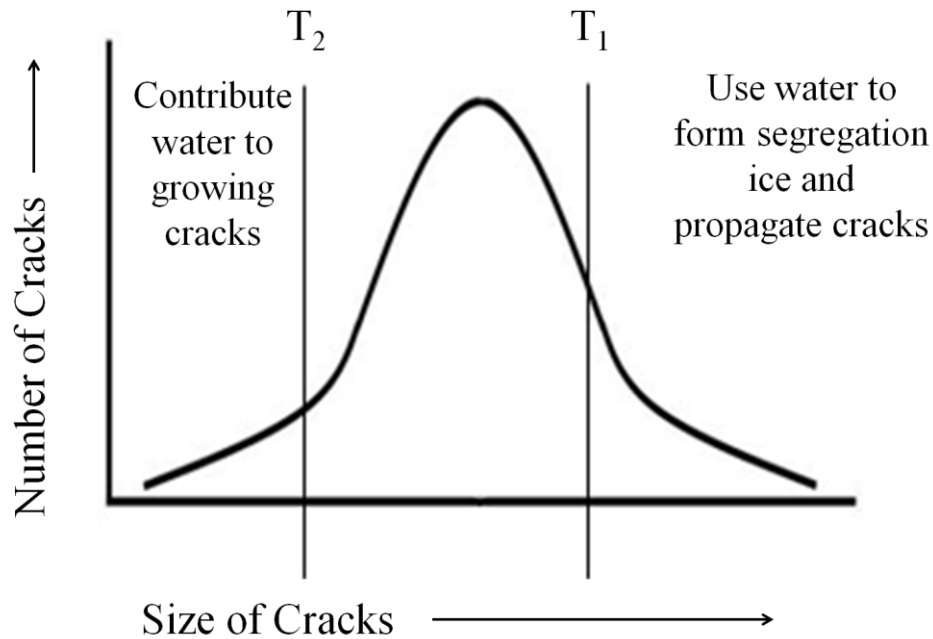


**Figure 10.** The distribution of crack lengths in a porous rock with two temperatures  $T_1$  and  $T_2$  denoted.  $T_1$  represents a temperature that is slightly below freezing and  $T_2$  represents a temperature that is well below freezing. The lines drawn on the normal crack distribution represent the threshold size of crack that temperature is able to propagate. Everything to the right of the temperature line is able to propagate, while everything to the left of the temperature line is giving up water to the segregation ice growing in large cracks.

occur if there is a sufficient number of cracks to the left and right of the threshold propagation length to both receive and supply premelted liquid.

The Eugene Formation is a sandstone that has many pores between grains and cement or within lithic grains that are available for pore fluid to saturate. These pores have a distribution of sizes that depend on the size and orientation of grains that surround them. To simplify the effects of pores in determining fracture propagation, the pores are treated as though they are crack-like flaws with a distribution of sizes. The crack size distribution in the sample cores used during my experiments was not detectable at the macroscopic level prior to freezing. In my rock coring experiments, I choose to core samples that had no visible signs of deformation before my experiments. Since the stress intensity factor is scaled with the length of the crack, rocks that are highly fractured in hand sample should be more susceptible to ice segregation related deformation.

The permeability of the rock decreases with decreasing temperature. As ice begins to form in the pores of a rock, the premelted fluids must flow around the ice crystals. As the ice crystals become larger and the premelted fluid volume decreases with decreasing temperature, the path of fluid becomes restricted and the permeability of the rock decreases. This is especially important in rock with large pores where the formation of large ice crystals can have a profound impact on the permeability of the rock. Rocks with smaller pores tend to be less affected by this process because premelted liquids are coating the surfaces of the particles and the ice.

## Berea Sandstone and Tyee Formation

The Berea Sandstone and the Tyee Formation were both negative for deformation at temperatures between -2 and -16 °C. The Berea Sandstone has a very mature composition with well-rounded grains of quartz that are well sorted. The Berea Sandstone has pores that are all approximately the same size due to the homogeneity of grain sizes. This distribution of pore sizes may have created a case in which the growth of segregation ice in large pores could not pirate water from smaller pores because they do not exist in the rock. Ice segregation under isothermal conditions also requires that an adequate distribution of pore sizes be available to the formation of segregation ice and premelted films.

The experimental results suggest that while ice segregation can occur under isothermal conditions, it is not as effective at deforming rock as ice segregation occurring in the presence a strong thermal gradient and a reservoir of liquid water. Previous experimental studies by Hallet et al. (1991) used Berea Sandstone for ice segregation studies. In these studies a thermal gradient was induced and a reservoir of liquid water was provided for segregation ice to grow. They found that the Berea Sandstone was susceptible to ice segregation under these conditions. Under isothermal conditions, the segregation ice may run out of liquid water before enough segregation ice can form to cause cracks to grow significantly. This would prevent the fracture of well cemented rocks by isothermal ice segregation.

Another explanation for why the Tyee Formation and Berea Sandstone did not show signs of deformation due to ice segregation is that the cement binding the grains

together in both of these sandstones is stronger than the pressure applied by the segregation ice. Increased rock strength will dramatically increase the critical stress intensity factor and make it more difficult for ice segregation to propagate cracks. The Eugene Formation is a very weak because the lithic fragments are weak and the clay films “cementing” the grains together are weak. The Tyee Formation sandstone is much stronger than the Eugene Formation sandstone due to the abundance of calcite cement. In the case of the Berea Sandstone, the grains and the cement were both composed of silica. This makes the Berea Sandstone very strong.

The Tyee Formation and Berea Sandstone may also have permeabilities much lower than the Eugene Formation. If the Tyee formation had a very low permeability, the premelted water may not have been able to migrate towards the growing segregation ice. The unfrozen permeability of the Berea Sandstone was large. After freezing occurred, the large pores within the Berea Sandstone may have filled with ice crystals and limited the flow of premelted water to growing segregation ice.

## CHAPTER V

### CONCLUSION

Laboratory results and thermal modeling rule out the presence of thermal shock and frost wedging in favor of a new, isothermal mode of ice segregation. This is the first laboratory evidence that conclusively shows that ice segregation can occur in the absence of a strong thermal gradient. This has important implications for understanding hazards associated with ice segregation because it means that ice segregation can occur throughout the winter in perpetually cold regions and not just during the spring and fall when thermal gradients are strong and a reservoir of liquid water is easily accessible. One type of solution engineers have come up with to avoid damage to structures from ice segregation is to keep permafrost and other cold regions refrigerated so they can not thaw out. One particular noteworthy example of this is in the Alaska Pipeline. Engineers have fixed the support beams with refrigeration units to keep the permafrost that the pipeline is built on from melting and deforming. This practice of keeping frozen objects frozen to prevent deformation may need to be reexamined if the material is poorly cemented rock or soil.

As seen in the case of the Berea Sandstone and the Tyee Formation, not all rocks are susceptible to isothermal ice segregation. The results of this study suggest that ice segregation occurs in very weak rocks and soils, consistent with previous studies of ice segregation as a mechanism for frost heave in weakly consolidated soils. The interpretation of ice segregation weathering needs to be carefully evaluated because there appears to be a broad range of thermal conditions that leads to deformation from ice

segregation. The erosion of soils, regolith and vegetation exposes fresh bedrock at the margins of glaciers. Glacial valleys have steep U-shaped valleys and steep headwalls near cirques that can provide bedrock at nearly isothermal conditions. The role of ice segregation in landscape evolution in cold regions should be investigated further.

Additional research needs to be conducted to better establish the physical parameters under which isothermal ice segregation can occur. The initial steps of this process would be to get polished sections of the Eugene formation, the Tyee Formation and the Berea Sandstone made with colored epoxy for analysis on the scanning electron microscope, SEM. The size, shape and distribution of the pores in all three sandstones could be evaluated using the SEM. More importantly, the influence of different amounts and types of cement needs to be assessed since it seems to be a major factor. A series of Tensile strength tests should be performed to evaluate the correlation between tensile strength and isothermal ice segregation susceptibility. Previous studies often use acoustic emissions, AE as a way of determining the exact timing and approximate location of cracking events. This would be a useful tool in collecting rock cracking data since the manual inspection of cores is tedious and only provides data at 15 minute time intervals. Developing the thermal model and incorporating a model that can accurately describe the flow of premelted liquids away from small cracks towards larger cracks will also be important in better understanding the isothermal ice segregation process.

## APPENDIX

### CORE COOLING MODEL DERIVATION

The thermal model of the Eugene Formation cores was developed to aid in understanding the fundamental processes occurring in the rock core during freezing. The equations are derived using the conservation of mass and energy. The flow of liquids through the rock core are derived from the Darcy equation. As ice forms within pores, the darcy transport decreases as the permeability of the rock core decreases. These equations will solve for the thermal profile of the rock at any given time after submersion in the circulating bath. **Equation 12** describes the change in temperature with time and is used when the rock has cooled to 0 ° C or colder and ice formation is releasing latent heat.

$$\frac{\partial T}{\partial t} \left( 1 + \frac{S_T \Delta T_f \phi \beta S_l}{\widetilde{\rho C} (T_m - T)} + \frac{S_T \Delta T_f \phi \beta S_l S_i (1 - \rho_i / \rho_l)}{\widetilde{\rho C} (T_m - T) \Gamma (1 - S_a)} \right) \approx \quad \text{[Equation 12]}$$

$$\frac{\rho_l C_l \alpha_{hy} \phi S_l^\alpha}{\widetilde{\rho C}} \frac{\partial P_l}{P_{l0}} \frac{\partial T}{\partial r} \frac{\partial T}{\partial r} + \frac{\alpha_{th}}{\widetilde{\rho C} r} \frac{\partial}{\partial r} \left( \frac{K_e}{K_{e0}} r \frac{\partial T}{\partial r} \right) + \frac{\alpha_{hy} S_T \Delta T_f \phi}{\widetilde{\rho C} \Gamma P_{l0} r} \frac{S_i}{1 - S_a} \frac{\partial}{\partial r} \left( S_l^\alpha r \frac{\partial P_l}{\partial r} \right)$$

**Equation 13** describes the change in pore fluid pressure as a function of time.

$$\frac{\partial P_l}{\partial t} = \frac{P_l}{T} \frac{\partial T}{\partial t} + \frac{1}{\Gamma S_a} \left[ \left( \frac{\rho_i}{\rho_l} - 1 \right) \frac{\beta S_l P_l}{T_m - T} \frac{\partial T}{\partial t} + \frac{\alpha_{hy} P_l}{P_{l0} r} \frac{\partial}{\partial r} \left( S_l^\alpha r \frac{\partial P_l}{\partial r} \right) \right] \quad \text{[Equation 13]}$$

**Equation 14** does not allow the amount of air within the rock core to move within the core or change with time.

$$\rho_a S_a = \text{Constant} \quad \text{[Equation 14]}$$

I can solve a simplified version of **Equations 12 and 13** when the temperature of the rock is greater than 0° C because there is no latent heat release. This is described by

**Equations 15 and 16.**

$$\frac{\partial T}{\partial t} \approx \frac{\rho_l C_l}{\bar{\rho} C} \frac{\alpha_{hy} \phi}{\rho_{l0} S_l^\alpha} \frac{\partial P_l}{\partial r} \frac{\partial T}{\partial r} + \frac{\alpha_{th}}{r} \frac{\partial}{\partial r} \left( \frac{K_e}{K_{e0}} r \frac{\partial T}{\partial r} \right) \quad [\text{Equation 15}]$$

$$\frac{\partial P_l}{\partial t} = \frac{P_l}{T} \frac{\partial T}{\partial t} + \frac{\alpha_{hy} P_l}{P_{l0} r} \frac{\partial}{\partial r} \left( S_l^{-\alpha} r \frac{\partial P_l}{\partial r} \right) \quad [\text{Equation 16}]$$

$$S_T = \frac{\rho_i L}{\bar{\rho} C_0 \Delta T_f} \quad \text{Stefan Number} \quad [\text{Equation 17}]$$

$$\tilde{\rho} C = \frac{\bar{\rho} C}{\bar{\rho} C_0} \quad \text{Dimensionless heat capacity} \quad [\text{Equation 18}]$$

$$\alpha_{th} = \frac{K_{e0}}{\bar{\rho} C_0} \quad \text{Thermal diffusivity} \quad [\text{Equation 19}]$$

$$\alpha_{hy} = \frac{K_0 P_{l0}}{\mu_l \phi} \quad \text{Hydraulic diffusivity} \quad [\text{Equation 20}]$$

$$\rho_a = \frac{P_a}{RT} \quad \text{Ideal gas law} \quad [\text{Equation 21}]$$

$$S_i = \left[ 1 - \left( \frac{\Delta T_f}{T_m - T} \right)^\beta \right] (1 - S_a) \quad \text{Ice saturation} \quad [\text{Equation 22}]$$

$$S_l = \left( \frac{\Delta T_f}{T_m - T} \right)^\beta (1 - S_a) \quad \text{Liquid Saturation} \quad [\text{Equation 23}]$$

$$\rho_a = P_a / RT \quad \text{Density of air} \quad [\text{Equation 24}]$$

$$\Gamma = \frac{\rho_i}{\rho_l} - \left( \frac{\rho_i}{\rho_l} - 1 \right) \frac{S_l}{1 - S_a} \quad \text{Variable used in equations} \quad [\text{Equation 25}]$$

$$P_l = P_a \quad [\text{Equation 26}]$$

Parameters that control thermal evolution of the rock core

Term	Parameter	Value	Units	Reference
$\rho_i$	Density of ice	916.7	Kg/m <sup>3</sup>	2
$\rho_l$	Density of water	1000	Kg/m <sup>3</sup>	2
$\rho_p$	Density of particles	2800	Kg/m <sup>3</sup>	3
$c_i$	Heat Capacity of ice	2090	J/Kg K	3
$c_l$	Heat Capacity of water	4217	J/Kg K	3
$c_a$	Heat Capacity of air	1000	J/Kg K	3
$c_p$	Heat Capacity of particles	800	J/Kg K	3
$C_i$	Specific heat of ice (constant P)	1.9 x 10 <sup>6</sup>	J/m <sup>3</sup> K	3
$C_l$	Specific heat of water (constant P)	4.2 x 10 <sup>6</sup>	J/m <sup>3</sup> K	2
$C_p$	Specific heat of particles (constant P)	1.5 x 10 <sup>6</sup>	J/m <sup>3</sup> K	3
$L$	Latent heat	3.34x 10 <sup>3</sup>	J/Kg	2
$K_i$	Thermal conductivity of ice	2.21	Kg m/s <sup>3</sup> K	3
$K_l$	Thermal conductivity of water	0.56	Kg m/s <sup>3</sup> K	3
$K_p$	Thermal conductivity of particles	2.0	Kg m/s <sup>3</sup> K	3
$K_a$	Thermal conductivity of air	0.026	Kg m/s <sup>3</sup> K	3
R	Gas constant	286.9	J/Kg K	
$k_o$	Saturated permeability (value for Chena Silt)	4.1 x 10 <sup>-17</sup>	m <sup>2</sup>	3
$\mu_l$	Viscosity of water	1.8E-3	Pa s	4
$r$	Radius of core	0.0122	m	*
$T_f$	Temperature at which ice starts melting	272.969	K	4
$T_m$	Bulk melting temperature of ice	273	K	1
$\phi$	Porosity	0.24		*
$\alpha$	Alpha (value for Chena Silt)	3.20		3
$\beta$	Beta(value for Chena Silt)	0.5		3
$T_f$	Temperature at which ice starts melting	272.969	K	4
$T_m$	Bulk melting temperature of ice	273	K	1
$T$	Temperature		K	
$t$	Time		s	
$V$	Volume		m <sup>3</sup>	
$S_i$	Saturation of ice			
$S_l$	Saturation of water			
$S_a$	Saturation of air			
$h_i$	Specific enthalpy of ice			
$h_l$	Specific enthalpy of water			
$h_p$	Specific enthalpy of particles			
$h_a$	Specific enthalpy of air			

**Table 4.** Values of constants used in the thermal model. The subscript “<sub>0</sub>” in the equations denotes a reference value. The references are as follows <sup>1</sup>(Style et al., 2011), <sup>2</sup>(Sheshukov and Nieber, 2011), <sup>3</sup>(Andersland and Ladanyi, 2004), <sup>4</sup>(Rempel, 2007). A \* indicates the value is derived from laboratory results.

## REFERENCES CITED

- Andersland, O. B., and B. Ladanyi (2004), *Frozen Ground Engineering*, John Wiley and Sons, Inc., Hoboken, New Jersey (2<sup>nd</sup> Edition).
- Coussy, O. (2005), Poromechanics of freezing materials, *J. Mech. Phys. Solids*, 53, 1689-1718, doi:10.1016/j.jmps.2005.04.001.
- Dash, J. G., A.W. Rempel, and J. S. Wettlaufer (2006), The physics of premelted ice and its geophysical consequences, *Rev. Mod. Phys.*, 78, 695-742, doi:10.1103/RevModPhys.78.695.
- Davidson, G. P., and J. F. Nye (1985), A photoelastic study of ice pressure in rock cracks, *Cold Reg. Sci. Technol.*, 11, 141-153 doi:10.1016/0165-232X(85)90013-8.
- Hansen-Goos, H., and J. S. Wettlaufer (2010), Theory of ice premelting in porous media, *Phys. Revs. E*, 031604-1-031604-13, doi:10.1103/PhysRevE.81.031604.
- Gruber, S., and W. Haeberli (2007), Permafrost in steep bedrock slopes and its temperature-related destabilization following climate change, *J. Geophys. Res.*, 112, F02S18, doi:10.1029/2006JF000547.
- Hall, K. (1999), The role of thermal stress fatigue in the breakdown of rock in cold regions, *Geomorphol.*, 31, 47-63, doi:10.1016/S0169-555X(99)00072-0.
- Hall, K., and M. André (2001), New insights into rock weathering from high-frequency rock temperature data: an Antarctic study of weathering by thermal stress, *Geomorphol.*, 41, 23-35, doi:10.1016/S0169-555X(01)00101-5.
- Hallet, B., J.S. Walder, and C.W. Stubbs (1991), Weathering by segregation ice growth in microcracks at sustained subzero temperatures: Verification from an experimental study using acoustic emissions, *Permafrost Periglac. Process.*, 2, 283-300, doi:10.1002/ppp.3430020404.
- Hallet, B., L. Hunter, and J. Bogen (1996), Rates of erosion and sediment evacuation by glaciers: A review of field data and their implications, *Global Planet. Change*, 12, 213-155, doi:10.1016/0921-8181(95)00021-6.
- Hallet, B. (2006), Why do freezing rocks break?, *Science*, 314, 1092-1093, doi:10.1126/science.1135200.

- Hales, T. C., and J. J. Roering (2005), Climate-controlled variations in scree production, Southern Alps, New Zealand, *Geol. Soc. Am.*, *33*, 701-704, doi:10.1130/G21528.
- Hales, T. C., and J. J. Roering (2007), Climatic controls on frost cracking and implications for the evolution of bedrock landscapes, *J. Geophys. Res.*, *112*, F02033, doi:10.1029/2006JF000616.
- Matsuoka, N. (2001), Direct observation of frost wedging in alpine bedrock, *Earth Surf. Process. Landforms*, *26*, 601-614, doi:10.1002/esp.208.
- McGreevy, J. P., and W. B. Whalley (1985), Rock moisture and frost weathering under natural and experimental conditions: a comparative discussion, *Arct. Alp. Res.*, *17*, 337-346, doi:10.2307/1551022.
- Rempel, A. (2007), Formation of ice lenses and frost heave, *J. Geophys. Res.*, *112*, F02S21, doi: 10.1029/2006JF000525.
- Sheshukov, A. Y., J. L. Nieber (2011), One-dimensional freezing of nonheaving unsaturated soil: Model formulation and similarity solution, *Water Resour. Res.*, *47*, W11519, doi:10.1029/2011WR010512.
- Style, R. W., S. L. Peppin, A. C. F. Cocks, and J. S. Wettlaufer (2011), Ice-lens formation and geometrical supercooling in soils and other colloidal materials, *Phys. Rev. E*, *84*, 041402, doi:10.1103/PhysRevE.84.041402.
- Taber, S. (1929), Frost heaving, *J. Geol.*, *37*, 428-461, doi:10.1086/623637.
- Vlahou, I., and M. G. Worster (2010), Ice growth in a spherical cavity of a porous medium, *J. Glaciol.*, *56*, 271-277, doi:10.3189/002214310791968494.
- Washburn, L. (1980), Permafrost features as evidence of climatic change, *Earth Sci. Rev.*, *15*, 327-402, doi:10.1016/0012-8252(80)90114-2.
- Walder, J., and B. Hallet (1985), A theoretical model of the fracture of rock during freezing, *Geol. Soc. Am. Bull.*, *96*, 336-346.
- Walder, J., and B. Hallet (1986), The physical basis of frost weathering: toward a more fundamental and unified perspective, *Arct. Alp. Res.*, *18*, 27-32, doi:10.2307/1551211.
- Wettlaufer, J. S., and M. G. Worster (2006), Premelting dynamics, *Annu. Rev. Fluid Mech.*, *38*, 427-452, doi:10.1146/annurev.fluid.37.061903.175758.